

Syndecan Promotes Axon Regeneration by Stabilizing Growth Cone Migration

Tyson J. Edwards¹ and Marc Hammarlund^{1,*}

¹Department of Genetics, Program in Cellular Neuroscience, Neurodegeneration and Repair, Yale University School of Medicine, BCMM 436E, 295 Congress Avenue, New Haven, CT 06510, USA

*Correspondence: marc.hammarlund@yale.edu

<http://dx.doi.org/10.1016/j.celrep.2014.06.008>

This is an open access article under the CC BY-NC-ND license (<http://creativecommons.org/licenses/by-nc-nd/3.0/>).

SUMMARY

Growth cones facilitate the repair of nervous system damage by providing the driving force for axon regeneration. Using single-neuron laser axotomy and *in vivo* time-lapse imaging, we show that syndecan, a heparan sulfate (HS) proteoglycan, is required for growth cone function during axon regeneration in *C. elegans*. In the absence of syndecan, regenerating growth cones form but are unstable and collapse, decreasing the effective growth rate and impeding regrowth to target cells. We provide evidence that syndecan has two distinct functions during axon regeneration: (1) a canonical function in axon guidance that requires expression outside the nervous system and depends on HS chains and (2) an intrinsic function in growth cone stabilization that is mediated by the syndecan core protein, independently of HS. Thus, syndecan is a regulator of a critical choke point in nervous system repair.

INTRODUCTION

Axon regeneration is mediated by growth cone migration, often across increased distances and unfamiliar landscapes. Regenerating growth cones face challenges not encountered during development, including extended migratory distances, altered extracellular environments, increased target selection complexity, and new physical barriers. *In vivo* time-lapse imaging reveals that regenerating growth cones are disorganized and take aberrant trajectories (Kerschensteiner et al., 2005; Pan et al., 2003; Ylera et al., 2009), suggesting that lack of sustained and directed migration is a major barrier to successful regeneration. In contrast to initial growth cone formation after injury (Bradke et al., 2012), relatively little is known about the molecular mechanisms that support sustained growth cone migration during regeneration. In particular, the intrinsic mechanisms that function within regenerating neurons to support stable and directed growth cone migration during regeneration are poorly understood.

Syndecans are transmembrane heparan sulfate proteoglycans (HSPGs), proteins characterized by posttranslational attachment of heparan sulfate (HS) chains at specific extracel-

lular serine residues. In general, HSPGs are thought to mediate interactions between extracellular ligands and their receptors via HS chains (Bernfield et al., 1999; Kramer and Yost, 2003; Lee and Chien, 2004). Consistent with this idea, HS binds multiple signaling molecules, including the morphogens Sonic Hedgehog, Wnts, and BMPs, insoluble extracellular matrix components such as fibronectin and laminin, and growth factors (Bernfield et al., 1999). Additionally, heparin—a closely related polysaccharide—makes ternary complexes with both fibroblast growth factor (FGF) and its receptor (Schlessinger et al., 2000; Yayon et al., 1991) and Slit/Robo (Hussain et al., 2006; Johnson et al., 2004). Thus, many signaling interactions with syndecan likely depend on HS chains. However, syndecan's protein core (alone among all HSPGs) includes conserved cytoplasmic domains (Bernfield et al., 1999), suggesting that some syndecan functions may be mediated by the protein itself rather than its heparan sulfate chains.

Syndecans are dynamically regulated by neuronal injury. Specifically, syndecan-1 mRNA is induced in the injured hypoglossal motor nucleus, along with the HS biosynthetic enzyme EXT-2, resulting in corresponding increases in HS expression in the motor nucleus and syndecan protein on the regenerating axons (Murakami and Yoshida, 2012; Murakami et al., 2006). Syndecan-1 and two HS-modifying enzymes are also increased in astrocytes after a cortical stab injury (Properzi et al., 2008). The dynamic regulation of syndecan after neuronal injury suggests that it may have important functions during axon regeneration. In *C. elegans*, a recent screen in posterior lateral microtubule mechanosensory axons identified syndecan as one of its strongest hits (Chen et al., 2011), and syndecan's role in regeneration was further validated in a screen for GABAergic neuron regeneration (Nix et al., 2014). However, how syndecan contributes to regenerative growth is unknown, and whether heparan sulfate itself promotes (Chau et al., 1999) or inhibits (Groves et al., 2005) axon regeneration remains unclear.

In order to address the role of syndecan after neuronal injury, we examined regeneration in *C. elegans* syndecan mutants using laser axotomy. We find that severed neurons in syndecan mutants fail to regenerate due to decreased growth cone stability. We conclude that syndecan has a function in growth cone stabilization during axon regeneration that is mechanistically distinct from its described role in axon guidance. Our results define syndecan as a regeneration factor and highlight the importance of sustained growth cone migration for successful axon regeneration.

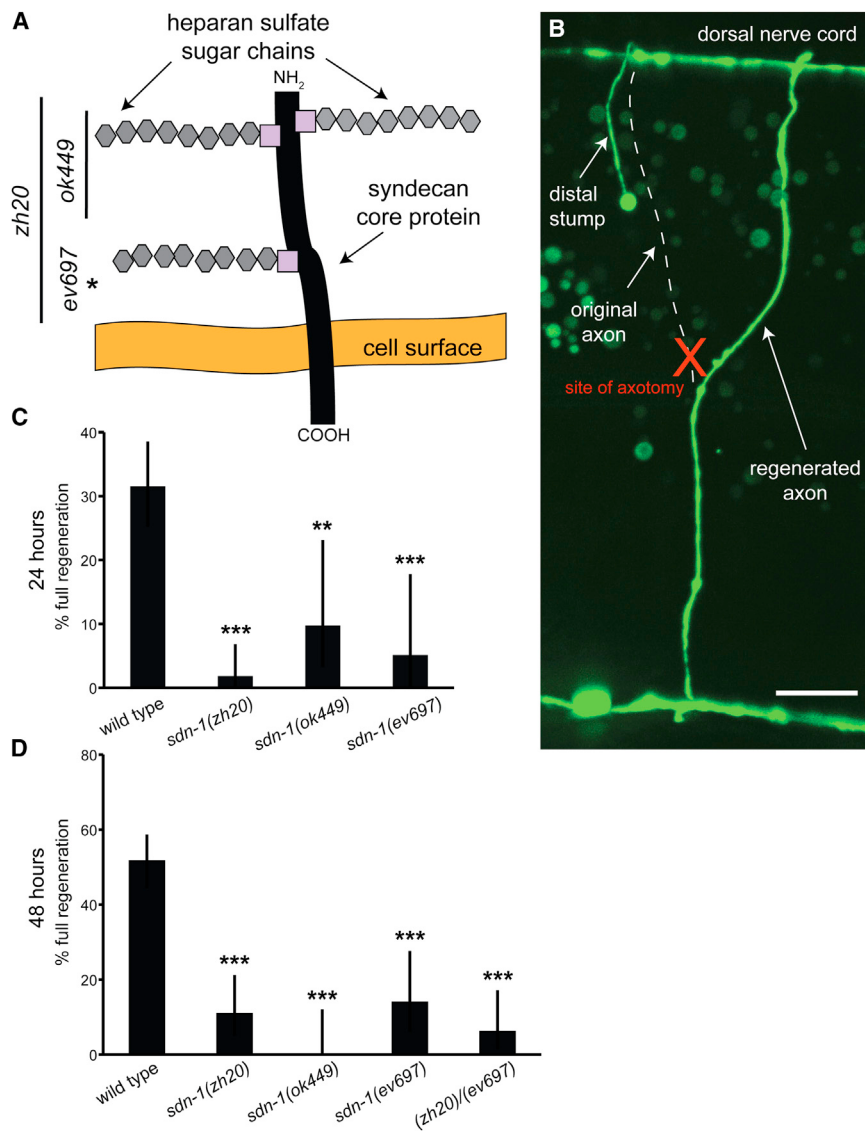


Figure 1. Syndecan Is Required for Axon Regeneration

(A) Syndecan is the only transmembrane HSPG and consists of long heparan sulfate sugar chains attached to a protein core. Three mutant syndecan alleles exist in *C. elegans*, including two deletion alleles that disrupt the extracellular sugar chains and a point mutation that induces a stop codon before the transmembrane domain. *sdn-1(zh20)* is the proposed null allele.

(B) Representative image of full regeneration after laser axotomy. Asterisk marks the remaining distal fragment. Dotted line indicates the approximate axonal trajectory before axotomy, and the red X marks the site of axotomy.

(C and D) Full regeneration is decreased in all three *sdn-1* alleles at 1 day (C) and 2 days (D) after axotomy. Syndecan transheterozygotes display reduced full regeneration 2 days after axotomy. Scale bars represent 10 μm. N(axons) ≥ 30 axons for all genotypes. Error bars represent 95% confidence intervals. **p < 0.005; ***p < 0.0005.

(Rhiner et al., 2005), as well as an enhancement of gonad patterning defects in an *unc-5*/Netrin receptor mutant background (Schwabiuk et al., 2009).

We severed GABAergic motor neurons with a pulsed dye laser in mutant and wild-type animals (Byrne et al., 2011). We assessed the ability of injured neurons to complete a relatively difficult and complex task: full regeneration back to the dorsal nerve cord, which requires growth cone initiation, sustained growth, and directed migration (Figure 1B). We found that 24 hr after injury, 32% of injured neurons in wild-type animals reach the dorsal cord (Figure 1C), consistent with previous results (El Bejjani and Hammarlund, 2012). By contrast, all three *sdn-1* alleles result in

a dramatic decrease in the number of severed axons that regenerate back to the dorsal cord in 24 hr (Figure 1C). To determine whether loss of syndecan blocks or merely delays regeneration, we assessed regeneration after 48 hr in all three alleles and in a *sdn-1* transheterozygote (Figure 1D). We found that this extra time increased the amount of regeneration to the dorsal cord in wild-type animals from 32% to 52% ($p < 0.0001$) but did not enable any additional regeneration in syndecan mutants ($p = 0.1385$, alleles pooled). Thus, syndecan is required for axon regeneration, and animals that lack syndecan fail to restore circuit connectivity after nerve injury.

A Long-Distance Enhancer May Regulate Syndecan Expression during Regeneration

We next attempted to rescue regeneration defects in *sdn-1* mutants. Because of previously reported difficulties in rescuing *sdn-1* mutants with high-copy transgenes (Rhiner et al., 2005;

RESULTS

Syndecan Is Required for Regeneration of the GABAergic Motor Neurons

In order to determine whether syndecan functions in axon regeneration *in vivo*, we examined axon regeneration in loss-of-function mutants in *sdn-1*, the sole *C. elegans* syndecan gene. We tested three *sdn-1* alleles (Figure 1A), including two deletion alleles, *sdn-1(ok449)* (Minniti et al., 2004) and *sdn-1(zh20)* (Rhiner et al., 2005), and a nonsense mutation, *sdn-1(ev697)* (Schwabiuk et al., 2009). All three *sdn-1* alleles are homozygous viable and are maintained as homozygotes. Further, the *sdn-1(zh20)* allele has been shown to be a null (Rhiner et al., 2005), as no *sdn-1* RNA is detected by northern blot in these animals. Thus, these animals enable the study of complete loss of syndecan function. All three *sdn-1* mutants display mild axon guidance defects in multiple neuron types, including the GABAergic motor neurons

Hannes Bülow, personal communication), we utilized the MosSci technique (Frøkjær-Jensen et al., 2012; Frøkjær-Jensen et al., 2008) to generate a single-copy insertion of a genomic clone of the wild-type *sdn-1* locus. We made two MosSci insertions, one containing 8 kb of highly conserved promoter region and the entire annotated *sdn-1* 3' UTR, the other a larger 15 kb construct including all of the 5' and 3' UTRs to the neighboring genes. We found that both insertions efficiently rescued the developmental axon guidance defects observed in *sdn-1* mutants. However, neither insertion significantly improved regeneration (data not shown). We also made a MosSci insertion expressing *sdn-1* from a neuron-specific promoter; this insertion only moderately rescued the guidance defects and also displayed no rescue of regeneration (data not shown). Finally, we tested the ability of previously described rescuing constructs (which partially rescue some axon guidance phenotypes) to restore regeneration and found that these also fail to rescue the axon regeneration defects (Rhiner et al., 2005). We conclude that unidentified, long-distance regulatory elements or genomic positional requirements may be necessary for achieving proper *sdn-1* expression levels during regeneration.

Growth Cones Collapse in Regenerating *sdn-1* Mutants

Our endpoint analysis demonstrated that syndecan was required for long-distance migration during regeneration. To determine in detail how syndecan affects regenerating axons, we performed *in vivo* time-lapse imaging in wild-type and *sdn-1* mutant animals. Regenerating GABAergic motor neurons were imaged at 4 min intervals in the period after axotomy when regenerating axons were most likely to exhibit active growth. We focused only on axons that initiated some growth activity during the imaging window and examined various phenotypes, including initiation of activity in the ventral stump, growth cone behavior, and regeneration to the dorsal muscle boundary (this anatomical boundary contains adhesion sites between the skin and muscle [Francis and Waterston, 1991] that impede growth cone migration toward the dorsal nerve cord [Knobel et al., 1999]). In total, our analysis of 61 wild-type and 47 *sdn-1* axons revealed a requirement for syndecan in preventing growth cone collapse and promoting high-speed migration.

In wild-type animals, most severed axons that initiated activity formed growth cones at or near the tip of the stump. These growth cones quickly migrated toward the dorsal side of the animal until reaching the dorsal muscles (Figure 2A; Movie S1). In total, 70% of wild-type axons migrated to the dorsal muscles within our imaging time window (Table S1), consistent with the robust growth observed in our 24 hr and 48 hr endpoint analysis (Figure 1). Fifteen percent formed growth cones that did not reach the dorsal muscles, and 13% exhibited some filament extension without forming a growth cone (Table S1). Thus, regeneration in wild-type animals is characterized by growth cone formation at the axon stump and robust migration.

By contrast, time-lapse analysis of regeneration in *sdn-1* mutants revealed a surprising and unique defect: decreased stability of growth cones (Figure 2B; Movies S2, S3, and S4). In fact, half of regenerating *sdn-1* axons that initially formed a growth cone exhibited at least one growth cone collapse, as compared to only 17% in wild-type worms (Figure 2C). To deter-

mine the effect of this increase in collapses on growth cone perdurance, we measured the duration of growth cones from the time of initiation until collapse or the end of acquisition. We found that growth cones in wild-type persisted for an average of 480 min, whereas those in *sdn-1* mutants lasted only 281 min (Figure 2D). Finally, we observed that while the start time to filamentous growth activity after injury was unchanged in *sdn-1* mutants (Figure 2E), initial growth cone formation was significantly delayed (Figure 2F). Growth cone destabilization severely impaired dorsal progression, as only 17% of *sdn-1* mutant axons reached the dorsal muscles during the analysis period (Table S1). Taken together, these data show that one of syndecan's primary roles is to stabilize growth cones and that decreased growth cone stability dramatically affects the final outcome of regeneration.

Syndecan Translates Growth Activity into Rapid Extension

To determine whether decreased growth cone stability affects the speed and efficiency of migration, we examined the effective regeneration growth rate by measuring the dorsal progression of the axon during periods of growth activity (Figures 3A and 3B). Activity was characterized by the initiation of sustained filamentous growth from the cut axon and proceeded until activity stopped or the axon reached the dorsal muscles (see *Supplemental Experimental Procedures*). We measured the distance from the ventral nerve cord to the dorsal-most point of the axon at the beginning and end of activity periods and then calculated the effective growth rate during that period (Figures 3C and 3D). We separated these activity events into two categories. Unproductive events were defined as events in which essentially no net growth occurred during the activity period (<5 μm net dorsal growth). These events tended to be of relatively short duration (wild-type [WT] mean = 100 min; *sdn-1* mean = 124 min) and were more common in *sdn-1* mutants (Figure 3E). Productive events, in which net dorsal growth did occur (>5 μm), were of relatively longer duration (WT mean = 197 min, p = 0.0003 versus WT unproductive; *sdn-1* mean = 284 min, p = 0.0008 versus *sdn-1* unproductive). During productive activity periods, wild-type axons progressed toward the dorsal nerve cord almost twice as fast as *sdn-1* mutant axons, whereas there was no change in the average rate of unproductive events (Figure 3F). We conclude that in addition to promoting growth cone stability and inhibiting collapse, syndecan has an important role in translating growth activity into directed migration.

Regenerating Axons in *sdn-1* Mutants Display Dysmorphic Growth

To confirm that the defects in *sdn-1* mutants were not caused by lengthy paralysis or repeated imaging associated with time-lapse analysis, we asked whether endpoint analysis could identify the growth cone defects observed in our time-lapse images. We recovered animals to normal conditions after surgery and analyzed regeneration approximately 24 hr later. In contrast to wild-type axons, which usually exhibit a growth cone structure that migrates toward the dorsal nerve cord (Figure 4A), we observed a broad range of dysmorphic phenotypes in *sdn-1* mutants, including small branches, long filaments, and malformed

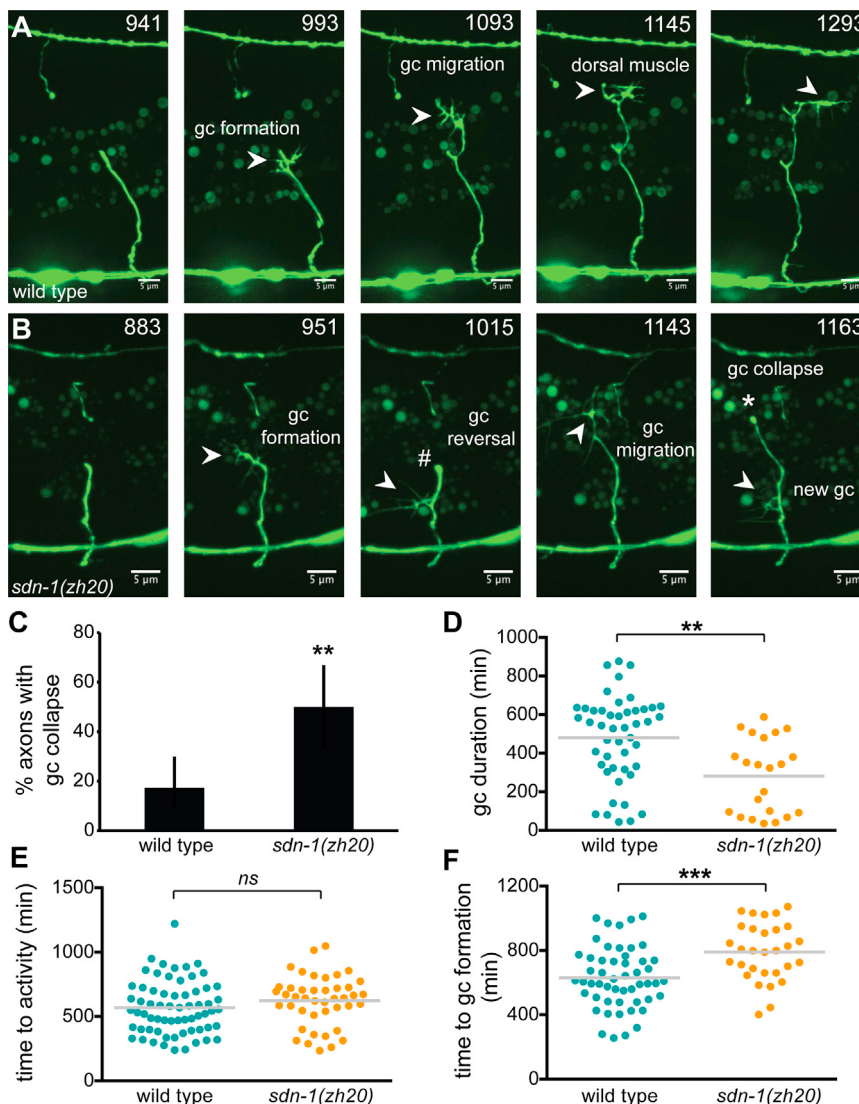


Figure 2. Syndecan Stabilizes Growth Cones during Regeneration

(A) Representative series of a regenerating axon in a wild-type worm from time-lapse analysis (see Movie S1). The growth cone forms and rapidly migrates toward the dorsal nerve cord. Once reaching the dorsal muscle boundary, the growth cone stalls and begins to branch out along the anterior-posterior axis but does not collapse.

(B) Representative time series of a regenerating *sdn-1* axon (see Movie S3). A growth cone forms at the tip and then turns back onto the proximal stump (#). It then grows actively toward the dorsal nerve cord but collapses (*) as new growth is initiated on the proximal stump. Arrowheads represent growth cones, and scale bars are 5 μm. Numbers in upper right indicate the time post-axotomy.

(C) Approximately three times as many axons exhibit growth cone collapse in *sdn-1* mutants. N(axons with growth cones) ≥ 30. Error bars represent 95% confidence intervals.

(D) The total duration of the growth cone from initiation to collapse or completion is decreased in *sdn-1* mutants. N(growth cones) > 20.

(E) Time to the start of the first activity period is not different between wild-type and *sdn-1* mutants. N(axons) > 40.

(F) The average time to growth cone initiation is increased in *sdn-1* mutants. N(axons with growth cones) ≥ 30. Dots represent individual events and horizontal lines represent the mean.

*p < 0.05; **p < 0.0005; ns, not significant. See Tables S1 and S2 for specific N values and statistics.

growth cone structures (Figures 4B and 4C). These dysmorphic growth structures are consistent with growth cone collapse and other dynamic behaviors observed during our time-lapse analysis. Other regenerating axons in *sdn-1* mutants looked grossly normal but often migrated only to the approximate midline (Figure 4D). Consistent with the dysmorphic growth and stunted migration in *sdn-1* mutants, we observed a significant decrease in the lengths of severed axons in *sdn-1* mutants (Figure 4E). These data are also consistent with the reduction in axons that successfully migrate to the dorsal nerve cord in *sdn-1* mutants (Figure 1C). We conclude that syndecan defects can be observed at single time points after axotomy and that growth cone defects in *sdn-1* mutants are independent of the imaging process.

Syndecan's Role in Stabilizing Growth Cones May Not Require Sugar Chains

Syndecan's glycosaminoglycan chains are heavily modified by a diverse group of heparan sulfate-modifying enzymes, including

sulfotransferases, an epimerase, and a sulfatase (Bernfield et al., 1999; Lee and Chien, 2004) (Figure 5A). The specific modifications made by each enzyme mediate specific roles in various aspects of *C. elegans* development and physiology, including axon guidance (Attreed et al., 2012; Bülow and Hobert, 2004; Townley and Bülow, 2011). In order to determine whether individual heparan sulfate sugar modifications are important for syndecan's function in axon regeneration, we examined loss-of-function mutants that lack individual modifying enzymes. We found that modifying enzyme mutants display wild-type levels of full regeneration (Figure 5B). Thus, individual modifications to syndecan's heparan sulfate chains, though required for development of the nervous system, are not required to promote growth cone migration after injury of the GABAergic motor neurons.

Since individual modifications to syndecan's HS chains are dispensable for regeneration, we asked whether the HS chains themselves are required for regeneration. Heparan sulfate chains are synthesized by multiple exostoses (EXT) family members (Esko and Selleck, 2002; Lee and Chien, 2004). In *C. elegans*, two EXT homologs exist (Clines et al., 1997), and at least one of these genes, *rib-2*, is necessary for HS biosynthesis

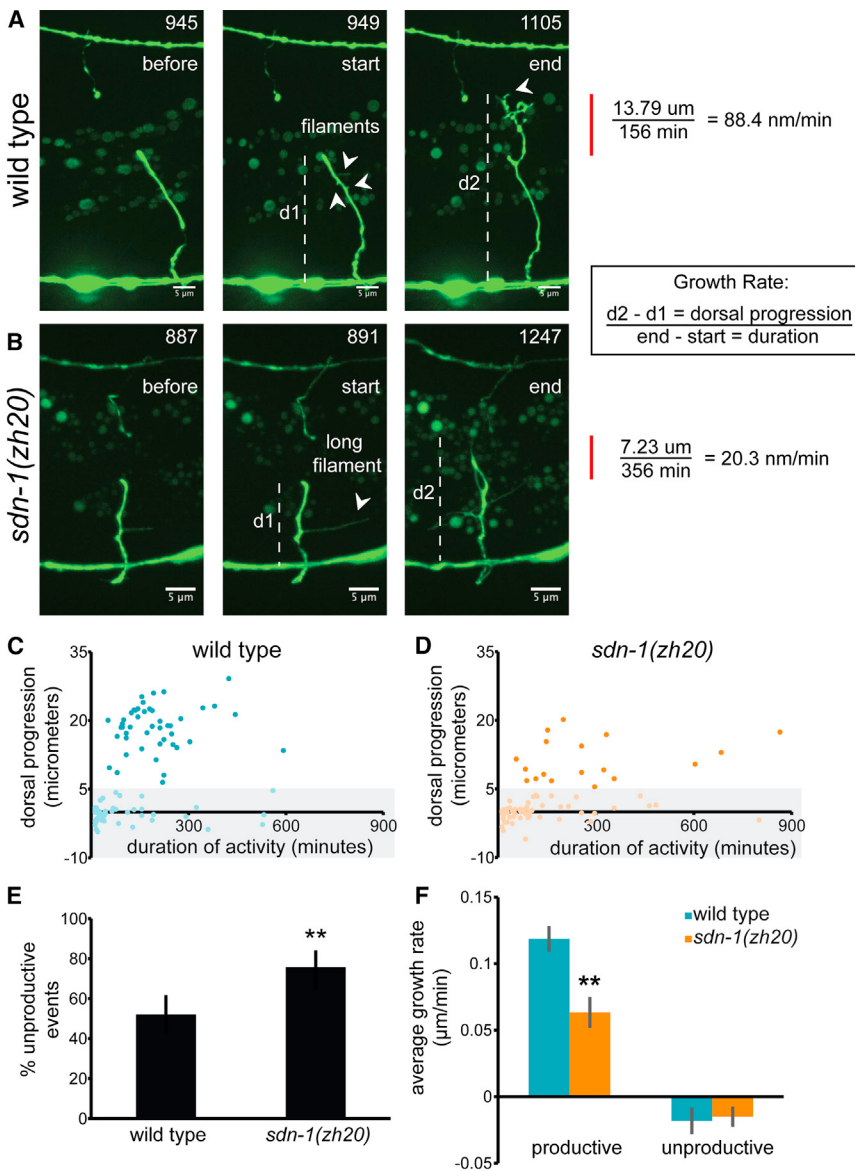


Figure 3. The Effective Growth Rate Is Reduced in *sdn-1* Mutants

(A–D) The growth rate was quantified by measuring the distance from the ventral nerve cord to the tip of the axon at the beginning and end of activity periods in wild-type (A; Movie S1) and *sdn-1* mutants (B; Movie S2). The first panel is before activity, the second panel is the start of activity, and the third panel is the end of activity. Dorsal progression (red bars) was divided by duration of growth to determine the effective migration rate. Dotted lines represent dorsal measurements, and arrowheads indicate filaments or branches. Scale bars represent 5 μm , and numbers in the upper right are minutes after axotomy. Duration of activity versus dorsal progression was plotted for wild-type (C) and *sdn-1* mutants (D). Each point represents one activity period. Shaded gray region represents unproductive activity periods with dorsal progression <5 μm .

(E) The proportion of unproductive events relative to all events is significantly increased in *sdn-1* mutants. N = 96 total events in wild-type and 74 events in *sdn-1*. Error bars represent 95% confidence intervals.

(F) The average growth rate for productive events is decreased by 47% in *sdn-1* mutants, whereas the average rate for unproductive events is unchanged from wild-type. Error bars represent $\pm\text{SEM}$.

** $p < 0.005$.

and viability (Kitagawa et al., 2001; Morio et al., 2003). We severed axons in *rib-2(gk318)* mutants isolated from balanced heterozygotes and observed normal rates of full regeneration to the dorsal cord as well as normal rates of partial regeneration, representing growth cone formation and migration close to the midline (Figures 5C and 5D). Interestingly, we did observe an increase in misguided regenerating axons in the *rib-2* mutants (Figure 5E), demonstrating that heparan sulfate is essential for axon guidance during regeneration, just as it is during neuronal development. Thus, we conclude that during regeneration, zygotically produced HS is required for axon guidance, but not for growth cone stability. However, it remains a possibility that maternally contributed *rib-2* could persist to mediate syndecan's role in growth cone stability, but not in axon guidance.

Two mammalian syndecan proteins are decorated with both heparan and chondroitin sulfate side chains (Deepa et al.,

2004; Rapraeger et al., 1985; Shwark et al., 1994). While *C. elegans* is devoid of chondroitin sulfate (Yamada et al., 1999), we investigated whether non-sulfated chondroitin plays a role in regeneration by examining the chondroitin synthase mutant *sqv-5* (Hwang et al., 2003; Mizuguchi et al., 2003). Similar to *rib-2* mutants, *sqv-5(n3611)* mutants are lethal and can be recovered from balanced heterozygotes. In *sqv-5*

homozygotes, we observed normal rates of full and partial regeneration 2 days after axotomy but also an increase in misguided regenerating growth cones (Figure S1). Thus, both heparan and chondroitin sugar chains appear to be required for guidance but dispensable (at least zygotically) for growth cone migration during axon regeneration. These experiments suggest that syndecan has two separable molecular roles: one in axon guidance, where syndecan functions via its modified HS chains (and potentially chondroitin) (Bülow and Hobert, 2004; Rhiner et al., 2005), and one in growth cone stability during axon regeneration. We propose that the syndecan core protein itself mediates growth cone stability during regeneration.

In a final effort to test whether syndecan's sugar chains mediate its regenerative function, we tested pathways that interact both genetically with syndecan and biochemically with

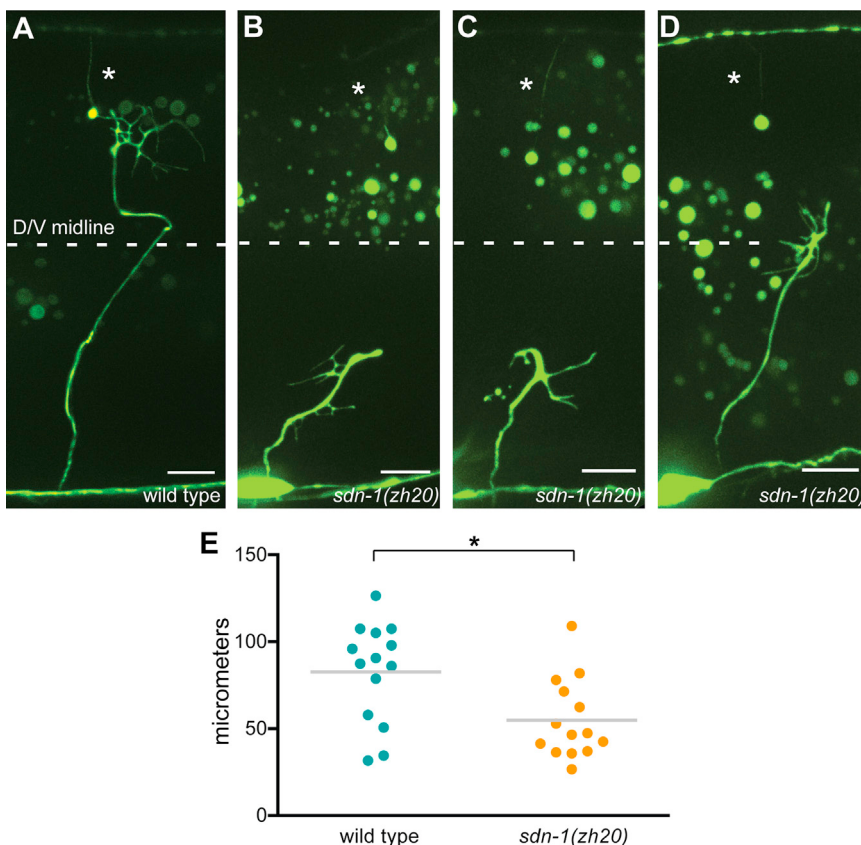


Figure 4. *sdn-1* Mutant Axons Display Dysmorphic Growth after Axotomy

(A) Representative image of regenerating growth cone in a wild-type animal.

(B and C) Images of dysmorphic growth in *sdn-1(zh20)* mutants. These mutant axons do not reach the midline.

(D) Regenerating axon in *sdn-1(zh20)* mutant is at the midline. Scale bars represent 10 μ m. Asterisks represent distal fragments. Dotted lines represent the approximate dorsal-ventral midline.

(E) Average regenerating neurite lengths are reduced in *sdn-1* mutants. Each dot represents a single axon, N = 14 axons. Horizontal lines represent the mean length. *p < 0.05.

acting in an HS-independent manner to promote growth cone migration during regeneration.

Syndecan Acts in Regenerating Neurons to Promote Sustained Migration

We next sought to determine where syndecan is functioning to promote the migration of regenerating growth cones. In *C. elegans*, syndecan is expressed in neurons and hypodermis (Minniti et al., 2004; Rhiner et al., 2005). Thus, syndecan could be acting directly in GABAergic motor neurons to promote

growth cone stability. Alternatively, syndecan could be acting nonautonomously in the hypodermis, which is the substrate for GABA neuron growth during development and regeneration.

To determine where syndecan functions, we subjected wild-type animals to *sdn-1* RNAi. *C. elegans* GABA neurons are resistant to RNAi (Asikainen et al., 2005; Calixto et al., 2010; Kamath et al., 2003; Timmons et al., 2001), and RNAi against *sdn-1* therefore generates animals in which *sdn-1* expression is maintained in GABA neurons but is depleted in other tissues. We found that syndecan RNAi animals recapitulated the developmental axon guidance defects present in the GABA neurons of *sdn-1* null mutants (Rhiner et al., 2005), including left-right axon guidance choices and migration toward the dorsal nerve cord (Figures 6A and 6B). These experiments show that syndecan RNAi animals are defective in syndecan guidance function at a level similar to that of null mutants and suggest that expression outside the GABA neurons (likely in the hypodermis) is essential for GABA axon guidance during development of the nervous system.

Next, we cut axons in syndecan RNAi animals and assessed regeneration. We found that syndecan RNAi animals, in contrast to *sdn-1* mutant alleles, were able to sustain wild-type levels of partial regeneration (Figure 6C). Thus, our results are consistent with the idea that GABA syndecan is sufficient to mediate growth cone stability and migration during regeneration. However, although regenerating axons in syndecan RNAi animals could sustain growth, they were often misguided in the anterior,

heparan sulfate. In particular, we investigated the Slit signaling pathway that directs axon guidance (Lee and Chien, 2004). Slit contains HS-binding sites, and heparin forms a ternary complex with Slit/Robo. Additionally, heparin is required for Slit-induced increases in growth cone collapse in vitro (Hussain et al., 2006). In *C. elegans*, there is a single Slit homolog, *slt-1*, that interacts with Robo/sax-3 (Hao et al., 2001) and the coreceptor eva-1 (Fujisawa et al., 2007) to direct neuronal development. Slit interacts with the same genetic pathway as syndecan for midline guidance of the PVQ interneurons, and GABAergic defects are no more severe in *sdn-1 slt-1* double mutants than in *sdn-1* alone (Rhiner et al., 2005). Likewise, the *hse-5*- and *hst-6*-modifying enzymes work with the Slit signaling pathway in guidance of the PVQ interneurons, and GABAergic defects are not enhanced or suppressed in the double mutant (Bülow and Hobert, 2004). Thus, developmental guidance of some neurons is likely mediated by Slit acting through HS chains on the syndecan core protein.

Because *sax-3* is thought to have *slt-1*-independent functions (Hao et al., 2001), we focused our investigation on *slt-1*. During regeneration, we observed normal levels of full regeneration in *slt-1(eh15)* mutants, which encodes a potential null allele of Slit (Hao et al., 2001), compared to wild-type (Figure 5F). Additionally, *slt-1* did not suppress the regeneration defects of *sdn-1* mutants (Figures 5G and 5H). Thus, we conclude that syndecan's effects on regeneration are not being mediated through Slit signaling. These data further support the idea that *sdn-1* is

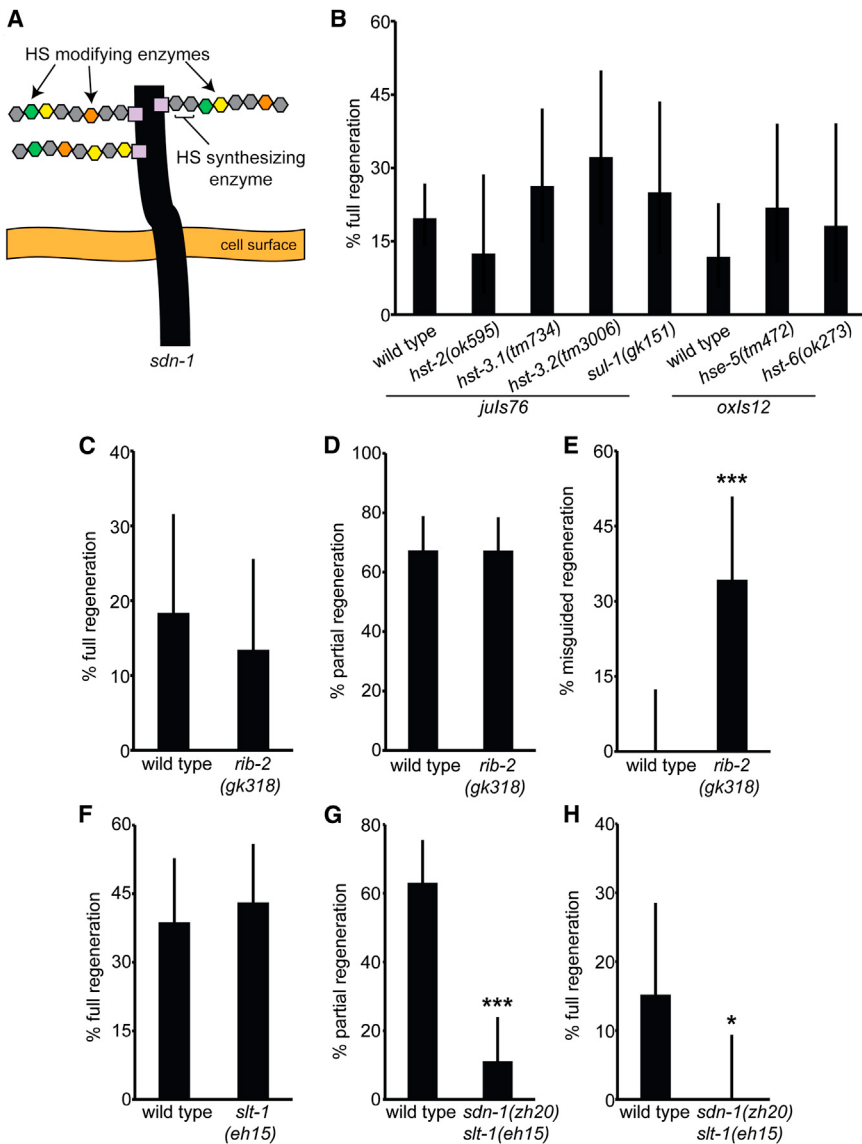


Figure 5. HSPG-Related Genes Are Not Required for Growth Cone Stability and Migration during Regeneration

(A) Schematic diagram of the syndecan protein with modified sugar residues (colored hexagons) formed by various modifying enzymes. Synthesizing enzymes extend the sugar chains by adding disaccharide units. Sugar chains are not to scale.

(B) The modifying enzymes do not show deficits in full regeneration after axotomy.

(C and D) The synthesizing enzyme *rib-2* displays normal full regeneration and partial regeneration after axotomy.

(E) *rib-2* mutants have an increased number of misguided regenerating axons.

(F) Full regeneration is not reduced in *slt-1(eh15)* animals.

(G and H) *sdn-1(zh20)slt-1(eh15)* double mutants display reduced partial and full regeneration.

N(axons) > 20 for all genotypes. Error bars represent 95% confidence intervals.

*p < 0.05, ***p < 0.0005.

to initiate, endure for shorter time periods, and are more prone to collapse, indicating a primary role for syndecan in stabilizing growth cones. These defects in growth cone stability limit the ability of regenerating axons to reconnect with their postsynaptic targets. Our data suggest that syndecan functions in neurons to promote growth cone stability during axon regeneration, whereas it functions in the hypodermis to promote axon guidance. Thus, regenerating axons must express syndecan to maintain growth cones, and failure to execute this genetic program results in growth cone collapse and failed regeneration (Figure 7B).

While a study of growth cone behavior in developing *sdn-1* neurons is lacking, we presume that defects in growth cone

stability are dramatically exacerbated during regeneration, as stunted, dysmorphic growth structures localized ventrally in uninjured *sdn-1* mutants are relatively rare (Rhiner et al., 2005; unpublished data). Thus, syndecan may have a distinct role in stabilizing growth cones postdevelopmentally when the extracellular environment has changed (Morgan et al., 2007).

Syndecan's neuronal role in stabilizing growth cones may be independent of HS sugar chains, in contrast to its HS-dependent function in axon guidance. HS binds multiple extracellular signaling molecules (Bernfield et al., 1999), including fibroblast growth factor (FGF) (Schlessinger et al., 2000; Yayon et al., 1991), Slit-Robo (Hussain et al., 2006), and Anosmin-1, a secreted protein involved in neurite outgrowth and branching (Hu et al., 2004; Soussi-Yanicostas et al., 1996, 1998, 2002). Genetic in vivo evidence suggests that syndecan interacts with these same signaling systems (Hudson et al., 2006; Johnson et al., 2004; Rhiner et al., 2005; Schwabiuk et al., 2009;

posterior, or ventral directions (Figure 6D and 6E), resulting in a decrease in the number of axons that regenerated fully to the dorsal nerve cord (Figure 6F). Thus, hypodermal syndecan is required to mediate syndecan's function in axon guidance (during development and regeneration). Overall, the regeneration phenotype of syndecan RNAi animals was similar to that of *rib-2* mutants, suggesting that hypodermal syndecan promotes the guidance of regenerating neurons via its HS sugar chains, while the neuronal function of syndecan in growth cone stability during regeneration is mediated by the syndecan core protein.

DISCUSSION

We have uncovered a role for the HSPG syndecan in promoting axon regeneration (Figure 7A). Although growth cones can form in response to injury in the absence of syndecan, they take longer

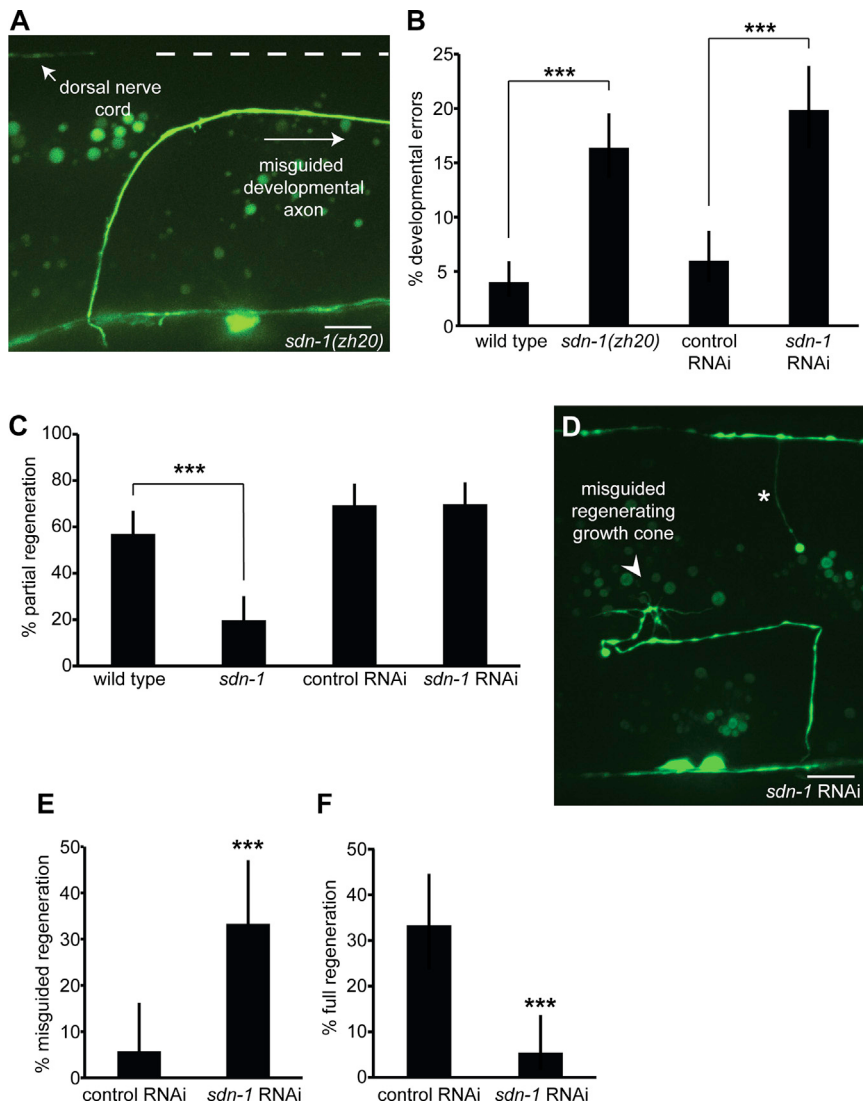


Figure 6. Growth Cone Formation and Migration Is Maintained in Syndecan-RNAi Animals

(A) An example of a developmental misguidance error in a *sdn-1(zh20)* animal. The axon migrated toward the dorsal nerve cord but then turned prematurely and migrated toward the tail. Arrowhead shows the dorsal nerve cord. Dotted line represents where the dorsal nerve cord should be located.

(B) Developmental errors, including left-right errors and migration defects, are increased in *sdn-1(zh20)* mutants and in wild-type worms on *sdn-1* RNAi. N(axons) > 400 for all genotypes in (A) and (B).

(C) Partial regeneration is significantly decreased in *sdn-1* mutants (*zh20* and *ev697* alleles pooled) after 24 hr, whereas it is the same in control versus *sdn-1* RNAi.

(D) Image of a misguided growth cone in a wild-type worm on *sdn-1* RNAi after laser axotomy. Arrowhead shows the growth cone. Asterisk marks the distal stump.

(E) Worms on *sdn-1* RNAi show an increase in misguided regenerating axons.

(F) Full regeneration is decreased in wild-type worms on *sdn-1* RNAi. N(axons) > 50 for all genotypes in (C), (E), and (F).

Scale bars represent 10 μ m. Error bars represent 95% confidence intervals. **p < 0.005, ***p < 0.0005.

Steigemann et al., 2004). Furthermore, heparan sulfate-synthesizing and modifying enzymes often phenocopy syndecan defects (Bülow and Hobert, 2004; Lee and Chien, 2004; Rhiner et al., 2005). However, there are precedents for HS-independent functions for the syndecan core protein. For example, the syndecan-4 core protein can induce the formation of stress fibers and adhesions even in a glycosylation-deficient cell line, indicating that overexpression of the core protein can bypass HS requirements (Echtermeyer et al., 1999). Syndecan is the only transmembrane HSPG, and the intracellular domain of syndecan contains conserved and variable regions that allow for interactions with a host of cytoplasmic signaling pathways (Bass et al., 2007, 2011; Bernfield et al., 1999; Hsueh et al., 1998; Kinnunen et al., 1998; Saoncella et al., 1999). Thus, while many of syndecan's functions likely depend on its heparan sulfate chains, evidence is emerging to suggest that the core protein itself has distinct functionality (Kramer and Yost, 2003; Van Vactor et al., 2006). Our data regarding HS-modifying and

HS-synthesizing enzymes, as well as *sli-1*, provide further evidence of this hypothesis.

We observe that growth cones form and retract on damaged axons in syndecan mutants, failing to sustain growth toward the dorsal nerve cord. One potential intracellular target of neuronal syndecan that might mediate growth cone stability is the axonal microtubule network. Microtubule remodeling at the growth cone is required for axon elongation and sustained migration (Bradke et al., 2012; Dent and Gertler, 2003; Ertürk et al., 2007; Vitriol and Zheng, 2012). Alternatively, syndecan could promote regeneration through adhesion pathways that modify actin filaments. Syndecans interact with several adhesive signaling systems including integrins, protein kinases, and the family of small Rho-GTPases (Morgan et al., 2007; Yoneda and Couchman, 2003). In culture, cells adhere to integrin-binding fragments of fibronectin but do not form actin stress fibers and focal adhesions unless stimulated with soluble heparan- or syndecan-binding fragments or syndecan-4 antibodies (Bass et al., 2007; Woods et al., 1986). The formation and regulation of adhesive contacts may be an essential step in sustained growth cone migration, and it could explain the regeneration defects we observe in *sdn-1* mutant worms.

The inability to rescue the syndecan regeneration defects with tissue-specific and native promoters suggests that *sdn-1* regulation is under tight transcriptional control. Though we have not

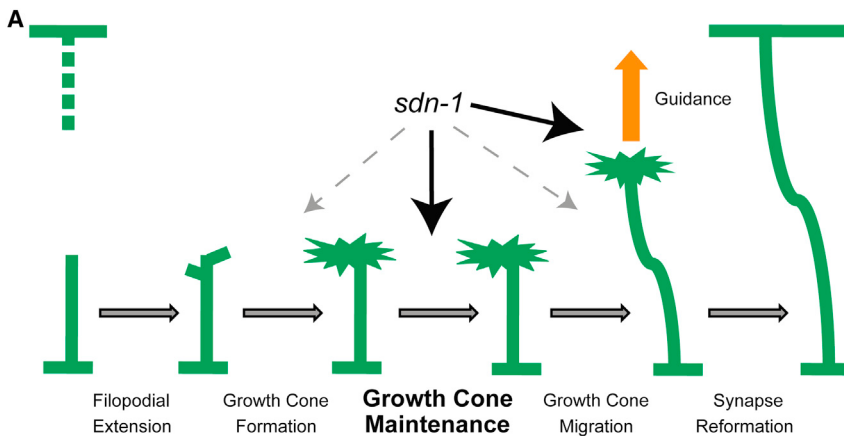
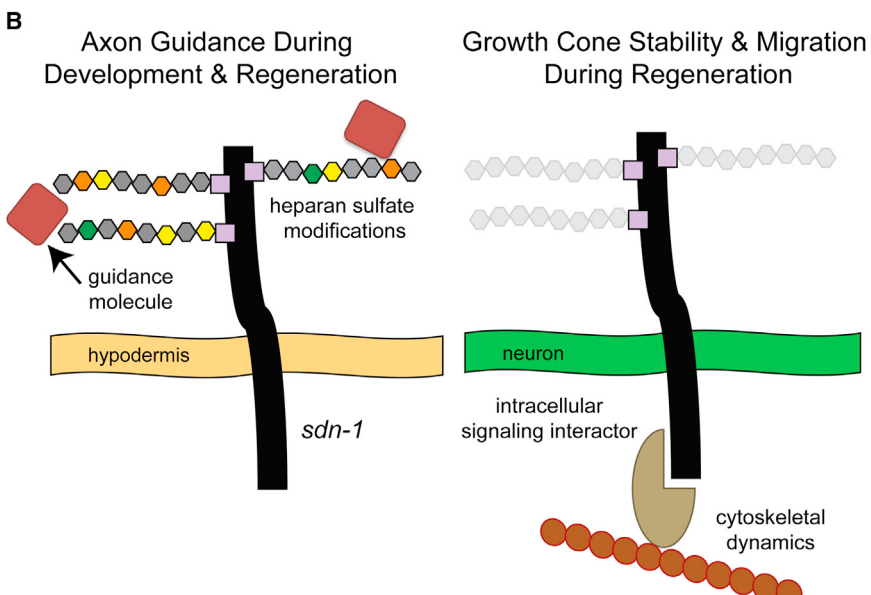


Figure 7. Model for Syndecan Function during Development and Regeneration

(A) Syndecan acts as a growth cone stabilizer to prevent collapse and drive efficient migration. It also guides axons to their preinjury targets. Other known regeneration factors affect growth cone formation or axon guidance.

(B) Syndecan is important for the guidance of axons during development and regeneration. Developmental guidance is mediated by several modifying enzymes. Guidance during regeneration is dependent on hypodermal expression of *sdn-1* and requires the HS synthesizing enzyme *rib-2*. Syndecan also plays an autonomous role in neurons to promote growth cone stability and migration. This function is independent of HS sugar chains and instead could rely on intracellular interactions that modulate the cytoskeleton.



tested *sdn-1* expression after axotomy in *C. elegans*, vertebrate syndecans are dynamically regulated in vivo (Bernfield et al., 1999; Kim et al., 1994), and expression is increased in both neuronal injury (Murakami and Yoshida, 2012; Murakami et al., 2006; Properzi et al., 2008) and skin-wounding models (Elenius et al., 1991). Additionally, wound-healing deficits have been reported in both syndecan-4 (Echtermeyer et al., 2001) and syndecan-1 (Stepp et al., 2002) mutant mice. Importantly, syndecan expression is activated by FGF application (Elenius et al., 1992; Jaakkola et al., 1997) through a long-range FGF-inducible response element (FiRE) contained in the syndecan 5' UTR (Jaakkola et al., 1997). FiRE is activated by different growth factors in a cell-type-specific manner (Jaakkola et al., 1998a; Rautava et al., 2003) and is upregulated specifically in migrating, but not proliferating, keratinocytes in vivo (Jaakkola et al., 1998b). Thus, syndecan can be regulated by a distant enhancer to specifically promote migration, suggesting that failed rescue of regeneration in *sdn-1* mutants may be due to a missing expression element.

We have shown that regeneration of individual GABAergic motor neurons requires the HSPG syndecan. Our findings are confirmed by recent regeneration screens in distinct neuron types (Chen et al., 2011; Nix et al., 2014), supporting the idea that syndecan is generally required during regeneration. Importantly, while most genes affecting regeneration in *C. elegans* modulate the frequency of growth cone formation or the length of extension, the growth cone collapse defects we describe are unique among regeneration phenotypes in *C. elegans* and argue that genetic pathways exist to promote aspects of axon regeneration that are not yet fully appreciated. Additionally, our time-lapse analysis demonstrates that it is possible to quantify distinct regeneration pheno-

types that may remain hidden by single-endpoint assays. Our work identifies growth cone maintenance as a critical choke point for axon regeneration, and it is consistent with the model that neuronal syndecan has an HS-independent mode of action in maintaining regenerating growth cones and promoting recovery of damaged neuronal circuits.

EXPERIMENTAL PROCEDURES

C. elegans Strains

Worm strains were maintained at 20°C or room temperature on nematode growth media (NGM) plates seeded with OP50 bacteria. The transgenes *oxIs12[Punc-47:gfp]* (McIntire et al., 1997) and *juls76[Punc-25:gfp]* (Jin et al., 1999) mark the GABAergic nervous system and were used as controls. *sdn-1* transheterozygotes were generated by mating *juls76;sdn-1(ev697)* males to 5- to 9-day-old adult *juls76;sdn-1(zh20)* worms that had likely exhausted all sperm cells. Genotyping after axotomy revealed that 20 out of 21 worms that were scored were definitely transheterozygotes. *rib-2* mutants survive only from balanced heterozygotes, and only homozygous progeny that lost the fluorescent balancer were analyzed for regeneration. The strains used in this study include *juls76* II, OH2629 *juls76*; *sul-1(gk151)*, OH2633

juls76; hst-2(ok595), EB460 juls76; sdn-1(zh20), EB752 hst-3.1(tm734); juls76, EB753 juls76; hst-3.2(tm3006), XE1236 juls76; sdn-1(ok449), XE1269 juls76; rib-2(gk318)/hT2[bli-4(e937)let-?(q782)qls48], XE1481 juls76; sdn-1(ev697), XE1007 oxls12, XE1677 sqv-5(n3611)/hT2[bli-4(e937) let-?(q782)qls48]; juls76, XE1680 juls76; sdn-1(zh20) slt-1(eh15), XE1235 juls76;slt-1(eh15), OH1510 hse-5(tm472); oxls12, and OH1179 hst-6(ok273); oxls12.

Axotomy

Axons (one to three per animal) were cut as previously described (Byrne et al., 2011; El Bejjani and Hammarlund, 2012). Approximate mid- to late-stage L4 hermaphrodite worms were immobilized in 50 mM muscimol or 50 nm polystyrene beads, with no noticeable differences between the two methods (El Bejjani and Hammarlund, 2012). Regeneration was typically assessed 1 day (approximately 18–24 hr) or 2 days (approximately 42–48 hr) postaxotomy, with an internal control done on the same day. Full regeneration represented axons that regenerated to the dorsal nerve cord. Partial regeneration represented axons that extended growth cones dorsally close to the midline or beyond, including full regeneration. Misguided regenerating axons were counted as the number of misguided axons divided by the number of total regenerating axons and represented instances where the growth cone extended but in anterior, posterior, or ventral directions, thus not necessarily reaching the midline or the dorsal cord.

For neurite tracing experiments, 1 μm z stack images were acquired at room temperature on an UltraVIEW Vex (PerkinElmer) spinning disc confocal microscope (Nikon Ti-E Eclipse inverted scope; Hamamatsu C9100-50 camera) with a 60× CFI Plan Apo numerical aperture (NA) 1.4 oil-immersion objective using Volocity software (Improvision). Images were exported as maximum-intensity projections and analyzed using ImageJ. The axons were traced from the ventral nerve cord up through all of the visible branches using the freehand tool. The distal stump length and worm diameter was also measured and was not statistically different between wild-type and control worms (data not shown). Axons that exhibited growth were quantified and compared using an unpaired t test.

Time-Lapse Imaging

We immobilized three to five worms simultaneously on 5%–7% agarose pads, mounted in ~1 μl of 50 nm polystyrene microbeads (Fang-Yen et al., 2012) spiked with 0.5–5 mM muscimol. The coverslip was sealed with Vaseline and mounted on an UltraVIEW VoX (PerkinElmer) spinning disc confocal microscope (Nikon Ti-E Eclipse inverted scope; Hamamatsu C9100-50 camera) with a 60× ApoTIRF 1.49 NA oil objective using Volocity (Improvision). We imaged regenerating axons at 60×, acquiring 1 μm z stacks every 4 min using the NikonTi Perfect Focus system. Images were compressed into maximum intensity projections, exported as stacked TIFFs, and processed using ImageJ. Movies were rotated, time stamped, and assigned a random number for analysis. Only axons that exhibited growth activity from the injured neuron were analyzed. See *Supplemental Experimental Procedures* for additional information on time-lapse analysis.

RNAi

We poured NGM plates with 25–50 μg/ml carbenicillin and 1 mM isopropyl β-D-1-thiogalactopyranoside and seeded them with HT115 cells containing L4440 empty-vector control (pPD129.36) or plasmid targeting *sdn-1* (ORFeome RNAi library F57C7.3). We also used *unc-22* (pLT61.1) for an RNAi efficiency control and GFP (pPD128.110) as a neuron-resistant control. We placed L2- to L3-stage worms on RNAi plates and then examined L4- or adult-stage animals from subsequent generations for developmental and regeneration phenotypes. Developmental defects were quantified in the seven posterior GABA commissures and were scored as defective if (1) the axon grew incorrectly on the left side of the worm, (2) the axon did not fully make it to the dorsal nerve cord, or (3) both grew on the incorrect side and failed to migrate to the dorsal nerve cord. Categories 2 and 3 were not observed in wild-type worms on control RNAi and are only rarely seen in wild-type strains. We also noted a slight decrease in fluorescent neuronal cell bodies in wild-type *juls76* worms on GFP RNAi compared to control RNAi (18.2 on L4440 versus 13.6 on GFP RNAi; $p < 0.0001$), suggesting that low levels of neuronal knock-down may be occurring.

Statistics

Experiments that compared the same mutant genotype and control strain were pooled for statistical analysis. In instances where multiple mutant strains are compared to the same control, all axons for the wild-type were also pooled before analysis to each individual mutant. Categorical data (full regeneration, partial regeneration, dysmorphic growth, etc.) was compared using a Fisher's exact test. Continuous data (neurite length, time to initiation, duration, etc.) was analyzed with an unpaired t test. p values were calculated with GraphPad QuickCalcs (<http://www.graphpad.com/quickcalcs/>). See Table S2 for all N values and statistics.

SUPPLEMENTAL INFORMATION

Supplemental Information includes Supplemental Experimental Procedures, one figure, two tables, and four movies and can be found with this article online at <http://dx.doi.org/10.1016/j.celrep.2014.06.008>.

AUTHOR CONTRIBUTIONS

Experiments were designed by T.J.E. and M.H. and carried out by T.J.E.

ACKNOWLEDGMENTS

Research in the Hammarlund laboratory is supported by the Beckman Foundation, the Ellison Medical Foundation, and the NIH (grant R01NS066082 to M.H. and grant T32GM007223 to T.E.).

Received: August 12, 2013

Revised: April 29, 2014

Accepted: June 5, 2014

Published: July 3, 2014

REFERENCES

- Asikainen, S., Vartiainen, S., Lakso, M., Nass, R., and Wong, G. (2005). Selective sensitivity of *Caenorhabditis elegans* neurons to RNA interference. *Neuroreport* 16, 1995–1999.
- Attried, M., Desbois, M., van Kuppevelt, T.H., and Bülow, H.E. (2012). Direct visualization of specifically modified extracellular glycans in living animals. *Nat. Methods* 9, 477–479.
- Bass, M.D., Roach, K.A., Morgan, M.R., Mostafavi-Pour, Z., Schoen, T., Muramatsu, T., Mayer, U., Ballestrem, C., Spatz, J.P., and Humphries, M.J. (2007). Syndecan-4-dependent Rac1 regulation determines directional migration in response to the extracellular matrix. *J. Cell Biol.* 177, 527–538.
- Bass, M.D., Williamson, R.C., Nunan, R.D., Humphries, J.D., Byron, A., Morgan, M.R., Martin, P., and Humphries, M.J. (2011). A syndecan-4 hair trigger initiates wound healing through caveolin- and RhoG-regulated integrin endocytosis. *Dev. Cell* 21, 681–693.
- Bernfield, M., Götte, M., Park, P.W., Reizes, O., Fitzgerald, M.L., Lincecum, J., and Zako, M. (1999). Functions of cell surface heparan sulfate proteoglycans. *Annu. Rev. Biochem.* 68, 729–777.
- Bradke, F., Fawcett, J.W., and Spira, M.E. (2012). Assembly of a new growth cone after axotomy: the precursor to axon regeneration. *Nat. Rev. Neurosci.* 13, 183–193.
- Bülow, H.E., and Hobert, O. (2004). Differential sulfations and epimerization define heparan sulfate specificity in nervous system development. *Neuron* 41, 723–736.
- Byrne, A.B., Edwards, T.J., and Hammarlund, M. (2011). In vivo Laser Axotomy in *C. elegans*. *J. Vis. Exp.*
- Calixto, A., Chelur, D., Topalidou, I., Chen, X., and Chalfie, M. (2010). Enhanced neuronal RNAi in *C. elegans* using SID-1. *Nat. Methods* 7, 554–559.
- Chau, C.H., Shum, D.K.Y., Chan, Y.S., and So, K.-F. (1999). Heparan sulphates upregulate regeneration of transected sciatic nerves of adult guinea-pigs. *Eur. J. Neurosci.* 11, 1914–1926.

- Chen, L., Wang, Z., Ghosh-Roy, A., Hubert, T., Yan, D., O'Rourke, S., Bowerman, B., Wu, Z., Jin, Y., and Chisholm, A.D. (2011). Axon regeneration pathways identified by systematic genetic screening in *C. elegans*. *Neuron* 71, 1043–1057.
- Clines, G.A., Ashley, J.A., Shah, S., and Lovett, M. (1997). The structure of the human multiple exostoses 2 gene and characterization of homologs in mouse and *Caenorhabditis elegans*. *Genome Res.* 7, 359–367.
- Deepa, S.S., Yamada, S., Zako, M., Goldberger, O., and Sugahara, K. (2004). Chondroitin sulfate chains on syndecan-1 and syndecan-4 from normal murine mammary gland epithelial cells are structurally and functionally distinct and cooperate with heparan sulfate chains to bind growth factors. A novel function to control binding of midkine, pleiotrophin, and basic fibroblast growth factor. *J. Biol. Chem.* 279, 37368–37376.
- Dent, E.W., and Gertler, F.B. (2003). Cytoskeletal dynamics and transport in growth cone motility and axon guidance. *Neuron* 40, 209–227.
- Echtermeyer, F., Baciu, P.C., Saoncella, S., Ge, Y., and Goetinck, P.F. (1999). Syndecan-4 core protein is sufficient for the assembly of focal adhesions and actin stress fibers. *J. Cell Sci.* 112, 3433–3441.
- Echtermeyer, F., Streit, M., Wilcox-Adelman, S., Saoncella, S., Denhez, F., Detmar, M., and Goetinck, P. (2001). Delayed wound repair and impaired angiogenesis in mice lacking syndecan-4. *J. Clin. Invest.* 107, R9–R14.
- El Bejjani, R., and Hammarlund, M. (2012). Notch signaling inhibits axon regeneration. *Neuron* 73, 268–278.
- Elenius, K., Vainio, S., Laato, M., Salmivirta, M., Thesleff, I., and Jalkanen, M. (1991). Induced expression of syndecan in healing wounds. *J. Cell Biol.* 114, 585–595.
- Elenius, K., Määttä, A., Salmivirta, M., and Jalkanen, M. (1992). Growth factors induce 3T3 cells to express bFGF-binding syndecan. *J. Biol. Chem.* 267, 6435–6441.
- Ertürk, A., Hellal, F., Enes, J., and Bradke, F. (2007). Disorganized microtubules underlie the formation of retraction bulbs and the failure of axonal regeneration. *J. Neurosci.* 27, 9169–9180.
- Esko, J.D., and Selleck, S.B. (2002). Order out of chaos: assembly of ligand binding sites in heparan sulfate. *Annu. Rev. Biochem.* 71, 435–471.
- Fang-Yen, C., Gabel, C.V., Samuel, A.D.T., Bargmann, C.I., and Avery, L. (2012). Laser microsurgery in *Caenorhabditis elegans*. In *Methods in Cell Biology*, J.H. Rothman and A. Singson, eds. (New York: Academic Press), pp. 177–206.
- Francis, R., and Waterston, R.H. (1991). Muscle cell attachment in *Caenorhabditis elegans*. *J. Cell Biol.* 114, 465–479.
- Frokjaer-Jensen, C., Davis, M.W., Hopkins, C.E., Newman, B.J., Thummel, J.M., Olesen, S.-P., Grunnet, M., and Jorgensen, E.M. (2008). Single-copy insertion of transgenes in *Caenorhabditis elegans*. *Nat. Genet.* 40, 1375–1383.
- Frokjaer-Jensen, C., Davis, M.W., Ailion, M., and Jorgensen, E.M. (2012). Improved Mos1-mediated transgenesis in *C. elegans*. *Nat. Methods* 9, 117–118.
- Fujisawa, K., Wrana, J.L., and Culotti, J.G. (2007). The slit receptor EVA-1 coactivates a SAX-3/Robo mediated guidance signal in *C. elegans*. *Science* 317, 1934–1938.
- Groves, M.L., McKeon, R., Werner, E., Nagarsheth, M., Meador, W., and English, A.W. (2005). Axon regeneration in peripheral nerves is enhanced by proteoglycan degradation. *Exp. Neurol.* 195, 278–292.
- Hao, J.C., Yu, T.W., Fujisawa, K., Culotti, J.G., Gengyo-Ando, K., Mitani, S., Moulder, G., Barstead, R., Tessier-Lavigne, M., and Bargmann, C.I. (2001). *C. elegans* slit acts in midline, dorsal-ventral, and anterior-posterior guidance via the SAX-3/Robo receptor. *Neuron* 32, 25–38.
- Hsueh, Y.-P., Yang, F.-C., Kharazia, V., Naisbitt, S., Cohen, A.R., Weinberg, R.J., and Sheng, M. (1998). Direct interaction of CASK/LIN-2 and syndecan heparan sulfate proteoglycan and their overlapping distribution in neuronal synapses. *J. Cell Biol.* 142, 139–151.
- Hu, Y., González-Martínez, D., Kim, S.-H., and Bouloux, P.M.G. (2004). Cross-talk of anosmin-1, the protein implicated in X-linked Kallmann's syndrome, with heparan sulphate and urokinase-type plasminogen activator. *Biochem. J.* 384, 495–505.
- Hudson, M.L., Kinnunen, T., Cinar, H.N., and Chisholm, A.D. (2006). *C. elegans* Kallmann syndrome protein KAL-1 interacts with syndecan and glypcan to regulate neuronal cell migrations. *Dev. Biol.* 294, 352–365.
- Hussain, S.-A., Piper, M., Fukuhara, N., Strohlic, L., Cho, G., Howitt, J.A., Ahmed, Y., Powell, A.K., Turnbull, J.E., Holt, C.E., and Hohenester, E. (2006). A molecular mechanism for the heparan sulfate dependence of slit-robo signaling. *J. Biol. Chem.* 281, 39693–39698.
- Hwang, H.-Y., Olson, S.K., Esko, J.D., and Horvitz, H.R. (2003). *Caenorhabditis elegans* early embryogenesis and vulval morphogenesis require chondroitin biosynthesis. *Nature* 423, 439–443.
- Jaakkola, P., Vihtinen, T., Määttä, A., and Jalkanen, M. (1997). Activation of an enhancer on the syndecan-1 gene is restricted to fibroblast growth factor family members in mesenchymal cells. *Mol. Cell. Biol.* 17, 3210–3219.
- Jaakkola, P., Määttä, A., and Jalkanen, M. (1998a). The activation and composition of FIRE (an FGF-inducible response element) differ in a cell type- and growth factor-specific manner. *Oncogene* 17, 1279–1286.
- Jaakkola, P., Kontusaari, S., Kauppi, T., Määttä, A., and Jalkanen, M. (1998b). Wound reepithelialization activates a growth factor-responsive enhancer in migrating keratinocytes. *FASEB J.* 12, 959–969.
- Jin, Y., Jorgensen, E., Hartwieg, E., and Horvitz, H.R. (1999). The *Caenorhabditis elegans* gene unc-25 encodes glutamic acid decarboxylase and is required for synaptic transmission but not synaptic development. *J. Neurosci.* 19, 539–548.
- Johnson, K.G., Ghose, A., Epstein, E., Lincecum, J., O'Connor, M.B., and Van Vactor, D. (2004). Axonal heparan sulfate proteoglycans regulate the distribution and efficiency of the repellent slit during midline axon guidance. *Curr. Biol.* 14, 499–504.
- Kamath, R.S., Fraser, A.G., Dong, Y., Poulin, G., Durbin, R., Gotta, M., Kanapin, A., Le Bot, N., Moreno, S., Sohrmann, M., et al. (2003). Systematic functional analysis of the *Caenorhabditis elegans* genome using RNAi. *Nature* 421, 231–237.
- Kerschensteiner, M., Schwab, M.E., Lichtman, J.W., and Misgeld, T. (2005). In vivo imaging of axonal degeneration and regeneration in the injured spinal cord. *Nat. Med.* 11, 572–577.
- Kim, C.W., Goldberger, O.A., Gallo, R.L., and Bernfield, M. (1994). Members of the syndecan family of heparan sulfate proteoglycans are expressed in distinct cell-, tissue-, and development-specific patterns. *Mol. Biol. Cell* 5, 797–805.
- Kinnunen, T., Kaksonen, M., Saarinen, J., Kalkkinen, N., Peng, H.B., and Rauvala, H. (1998). Cortactin-Src kinase signaling pathway is involved in N-syndecan-dependent neurite outgrowth. *J. Biol. Chem.* 273, 10702–10708.
- Kitagawa, H., Egusa, N., Tamura, J.I., Kusche-Gullberg, M., Lindahl, U., and Sugahara, K. (2001). rib-2, a *Caenorhabditis elegans* homolog of the human tumor suppressor EXT genes encodes a novel α 1,4-N-acetylgalactosaminyltransferase involved in the biosynthetic initiation and elongation of heparan sulfate. *J. Biol. Chem.* 276, 4834–4838.
- Knobel, K.M., Jorgensen, E.M., and Bastiani, M.J. (1999). Growth cones stall and collapse during axon outgrowth in *Caenorhabditis elegans*. *Development* 126, 4489–4498.
- Kramer, K.L., and Yost, H.J. (2003). Heparan sulfate core proteins in cell-cell signaling. *Annu. Rev. Genet.* 37, 461–484.
- Lee, J.-S., and Chien, C.-B. (2004). When sugars guide axons: insights from heparan sulphate proteoglycan mutants. *Nat. Rev. Genet.* 5, 923–935.
- McIntire, S.L., Reimer, R.J., Schuske, K., Edwards, R.H., and Jorgensen, E.M. (1997). Identification and characterization of the vesicular GABA transporter. *Nature* 389, 870–876.
- Minniti, A.N., Labarca, M., Hurtado, C., and Brandan, E. (2004). *Caenorhabditis elegans* syndecan (SDN-1) is required for normal egg laying and associates with the nervous system and the vulva. *J. Cell Sci.* 117, 5179–5190.
- Mizuguchi, S., Uyama, T., Kitagawa, H., Nomura, K.H., Dejima, K., Gengyo-Ando, K., Mitani, S., Sugahara, K., and Nomura, K. (2003). Chondroitin

- proteoglycans are involved in cell division of *Caenorhabditis elegans*. *Nature* 423, 443–448.
- Morgan, M.R., Humphries, M.J., and Bass, M.D. (2007). Synergistic control of cell adhesion by integrins and syndecans. *Nat. Rev. Mol. Cell Biol.* 8, 957–969.
- Morio, H., Honda, Y., Toyoda, H., Nakajima, M., Kurosawa, H., and Shirasawa, T. (2003). EXT gene family member rib-2 is essential for embryonic development and heparan sulfate biosynthesis in *Caenorhabditis elegans*. *Biochem. Biophys. Res. Commun.* 301, 317–323.
- Murakami, K., and Yoshida, S. (2012). Nerve injury induces the expression of syndecan-1 heparan sulfate proteoglycan in peripheral motor neurons. *Neurosci. Lett.* 527, 28–33.
- Murakami, K., Namikawa, K., Shimizu, T., Shirasawa, T., Yoshida, S., and Kiyama, H. (2006). Nerve injury induces the expression of EXT2, a glycosyltransferase required for heparan sulfate synthesis. *Neuroscience* 141, 1961–1969.
- Nix, P., Hammarlund, M., Hauth, L., Lachnit, M., Jorgensen, E.M., and Bastiani, M. (2014). Axon regeneration genes identified by RNAi screening in *C. elegans*. *J. Neurosci.* 34, 629–645.
- Pan, Y.A., Misgeld, T., Lichtman, J.W., and Sanes, J.R. (2003). Effects of neurotoxic and neuroprotective agents on peripheral nerve regeneration assayed by time-lapse imaging *in vivo*. *J. Neurosci.* 23, 11479–11488.
- Properzi, F., Lin, R., Kwok, J., Naidu, M., van Kuppevelt, T.H., Ten Dam, G.B., Camargo, L.M., Raha-Chowdhury, R., Furukawa, Y., Mikami, T., et al. (2008). Heparan sulphate proteoglycans in glia and in the normal and injured CNS: expression of sulphotransferases and changes in sulphation. *Eur. J. Neurosci.* 27, 593–604.
- Rapraeger, A., Jalkanen, M., Endo, E., Koda, J., and Bernfield, M. (1985). The cell surface proteoglycan from mouse mammary epithelial cells bears chondroitin sulfate and heparan sulfate glycosaminoglycans. *J. Biol. Chem.* 260, 11046–11052.
- Rautava, J., Soukka, T., Heikinheimo, K., Miettinen, P.J., Happonen, R.-P., and Jaakkola, P. (2003). Different mechanisms of syndecan-1 activation through a fibroblast-growth-factor-inducible response element (FiRE) in mucosal and cutaneous wounds. *J. Dent. Res.* 82, 382–387.
- Rhiner, C., Gysi, S., Fröhli, E., Hengartner, M.O., and Hajnal, A. (2005). Syndecan regulates cell migration and axon guidance in *C. elegans*. *Development* 132, 4621–4633.
- Saconcella, S., Echtermeyer, F., Denhez, F., Nowlen, J.K., Mosher, D.F., Robinson, S.D., Hynes, R.O., and Goetinck, P.F. (1999). Syndecan-4 signals cooperatively with integrins in a Rho-dependent manner in the assembly of focal adhesions and actin stress fibers. *Proc. Natl. Acad. Sci. USA* 96, 2805–2810.
- Schlessinger, J., Plotnikov, A.N., Ibrahim, O.A., Eliseenkova, A.V., Yeh, B.K., Yayon, A., Linhardt, R.J., and Mohammadi, M. (2000). Crystal structure of a ternary FGF-FGFR-heparin complex reveals a dual role for heparin in FGFR binding and dimerization. *Mol. Cell* 6, 743–750.
- Schwabiuk, M., Coudiere, L., and Merz, D.C. (2009). SDN-1/syndecan regulates growth factor signaling in distal tip cell migrations in *C. elegans*. *Dev. Biol.* 334, 235–242.
- Shworak, N.W., Shirakawa, M., Mulligan, R.C., and Rosenberg, R.D. (1994). Characterization of ryudocan glycosaminoglycan acceptor sites. *J. Biol. Chem.* 269, 21204–21214.
- Soussi-Yanicostas, N., Hardelin, J.P., Arroyo-Jimenez, M.M., Ardouin, O., Legouis, R., Levilliers, J., Traincard, F., Betton, J.M., Cabanié, L., and Petit, C. (1996). Initial characterization of anosmin-1, a putative extracellular matrix protein synthesized by definite neuronal cell populations in the central nervous system. *J. Cell Sci.* 109, 1749–1757.
- Soussi-Yanicostas, N., Faivre-Sarrailh, C., Hardelin, J.P., Levilliers, J., Rougon, G., and Petit, C. (1998). Anosmin-1 underlying the X chromosome-linked Kallmann syndrome is an adhesion molecule that can modulate neurite growth in a cell-type specific manner. *J. Cell Sci.* 111, 2953–2965.
- Soussi-Yanicostas, N., de Castro, F., Julliard, A.K., Perfettini, I., Chédotal, A., and Petit, C. (2002). Anosmin-1, defective in the X-linked form of Kallmann syndrome, promotes axonal branch formation from olfactory bulb output neurons. *Cell* 109, 217–228.
- Steigemann, P., Molitor, A., Fellert, S., Jäckle, H., and Vorbrüggen, G. (2004). Heparan sulfate proteoglycan syndecan promotes axonal and myotube guidance by slit/robo signaling. *Curr. Biol.* 14, 225–230.
- Stepp, M.A., Gibson, H.E., Gala, P.H., Iglesia, D.D.S., Pajoohesh-Ganji, A., Pal-Ghosh, S., Brown, M., Aquino, C., Schwartz, A.M., Goldberger, O., et al. (2002). Defects in keratinocyte activation during wound healing in the syndecan-1-deficient mouse. *J. Cell Sci.* 115, 4517–4531.
- Timmons, L., Court, D.L., and Fire, A. (2001). Ingestion of bacterially expressed dsRNAs can produce specific and potent genetic interference in *Caenorhabditis elegans*. *Gene* 263, 103–112.
- Townley, R.A., and Bülow, H.E. (2011). Genetic analysis of the heparan modification network in *Caenorhabditis elegans*. *J. Biol. Chem.* 286, 16824–16831.
- Van Vactor, D., Wall, D.P., and Johnson, K.G. (2006). Heparan sulfate proteoglycans and the emergence of neuronal connectivity. *Curr. Opin. Neurobiol.* 16, 40–51.
- Vitriol, E.A., and Zheng, J.Q. (2012). Growth cone travel in space and time: the cellular ensemble of cytoskeleton, adhesion, and membrane. *Neuron* 73, 1068–1081.
- Woods, A., Couchman, J.R., Johansson, S., and Höök, M. (1986). Adhesion and cytoskeletal organisation of fibroblasts in response to fibronectin fragments. *EMBO J.* 5, 665–670.
- Yamada, S., Van Die, I., Van den Eijnden, D.H., Yokota, A., Kitagawa, H., and Sugahara, K. (1999). Demonstration of glycosaminoglycans in *Caenorhabditis elegans*. *FEBS Lett.* 459, 327–331.
- Yayon, A., Klagsbrun, M., Esko, J.D., Leder, P., and Ornitz, D.M. (1991). Cell surface, heparin-like molecules are required for binding of basic fibroblast growth factor to its high affinity receptor. *Cell* 64, 841–848.
- Ylera, B., Ertürk, A., Hellal, F., Nadrigny, F., Hurtado, A., Tahirovic, S., Oudega, M., Kirchhoff, F., and Bradke, F. (2009). Chronically CNS-injured adult sensory neurons gain regenerative competence upon a lesion of their peripheral axon. *Curr. Biol.* 19, 930–936.
- Yoneda, A., and Couchman, J.R. (2003). Regulation of cytoskeletal organization by syndecan transmembrane proteoglycans. *Matrix Biol.* 22, 25–33.